DOI 10.59277/RoAJ.2025.3.03

ATMOSPHERIC MODELING OF SOLAR-LIKE STAR τ CETI

FARAHHATI MUMTAHANA[1], A. LAKSANA[2]

[1]*Research Center for Space, National Research and Innovation Agency, Bandung, Indonesia*
[2]*Ahmad Dahlan University, Yogyakarta, Indonesia*
Email*: farahhati.mumtahana@brin.go.id*

Abstract. τ Ceti is a G-type main-sequence star (spectral type G8 V) and a member of Population II. Because of its proximity, similarity to the Sun, and the presence of a planetary system, it has long served as a benchmark object in stellar astrophysics. Its fundamental parameters have been extensively determined through observational surveys, theoretical analyses, and interior structure modeling. In this study, we focus on the atmospheric modeling of τ Ceti. Whereas interior models are primarily constrained by global properties such as stellar radius and mass, the atmospheric model provides access to the detailed thermodynamic structure of the star. In particular, we examine the variation of mass depth, temperature, pressure, density, and electron number density as functions of Rosseland optical depth (τ_R), thereby establishing a self-consistent framework for characterizing the stellar atmosphere. This framework further enables the generation of synthetic spectra, which can be directly compared with observational data to test the validity of the model.

Key words: Stellar Physics – Astrophysics – Stellar Atmosphere.

1. INTRODUCTION

Tau Ceti (HD 10700) is a metal-poor, Population II, G8V main-sequence star with an apparent magnitude of V = 3.50 $\pm$ 0.01 and an absolute magnitude of M_V = 5.69 $\pm$ 0.01 (**?**). Located at a distance of $3.65 \pm\ 0.01$ pc (**?**), it is one of the nearest solar-type stars, with an estimated age of 10.0 $\pm$ 0.5 Gyr (**?**). A nearby companion at a 10-arcsecond separation and magnitude 13.1 does not significantly impact measurements (**?**). The star exhibits a rotation period of approximately 34-46 days, with minimal modulation, suggesting a Maunder minimum-like state (**??**), and shows solar-like oscillations in its convective envelope. Structurally, it closely resembles the Sun, especially in terms of its hydrogen core (**?**).

? refine its physical parameters from interferometric and spectroscopic measurements, obtaining several parameters such as a limb-darkened angular diameter, radius, effective temperature, $\log g$, and a projected rotational velocity (Table **??**). These imply a nearly pole-on inclination of $7^\circ \pm\ 7^\circ$, which carries important implications for the true planetary masses in the system, as well as for the dynamical interpretation of the disk-stellar spin alignment **?**.

? initiated the study of τ Ceti by capturing an image revealing a dusty disk around the star, with a mass greater than that of the Kuiper Belt. Subsequent observations extended into the millimeter wavelength range using ALMA, as reported by **?**. While **?** initially proposed that τ Ceti hosts a five-planet system, more recent data from **?** refined this to four confirmed planets, with several parameters measured with reasonable certainty. The analysis employs the Radial Velocity (RV) method, incorporating a moving average model to handle wavelength-dependent noise, known as “differential radial velocity”. **?**'s model enhances the HARPS (High Accuracy Radial Velocity Planet Searcher) data, which were earlier analyzed by **?** under the MT13 project.

Previous studies have investigated the fundamental parameters of τ Ceti through spectroscopy, interferometry, and interior structure modeling constructed with MESA (**?**), using several key parameters derived from recent observations. The primary objective of this work is to conduct a detailed analysis of the stellar atmosphere of τ Ceti using MARCS model atmospheres. Owing to its proximity, well-characterized parameters, and solar-like properties, τ Ceti serves as an ideal benchmark for high-precision atmospheric modeling. The analysis adopts an approach analogous to interior modeling, but rather than focusing on global parameters such as stellar radius, the atmospheric model examines the stratification of thermodynamic quantities-including mass depth, temperature, pressure, density, and electron number density-as functions of Rosseland optical depth ($\tau_{\rm Ross}$). This provides a comprehensive description of the stellar atmosphere, complementing existing knowledge of τ Ceti's internal structure. In addition, synthetic spectra generated from these models enable direct comparisons with spectroscopic observations, offering a means to test and validate atmospheric models and refine stellar parameter determinations.

2. PHYSICAL PROPERTIES OF τ CETI

Table **??** presents the adopted stellar parameters together with their respective references. These parameters provide the basis for constructing a MARCS-based atmospheric model, which is essential for achieving reliable spectroscopic analyses, particularly in the context of chemical abundance determinations and stellar activity. The resulting model thus establishes a solid framework for future studies of τ Ceti and other nearby solar-type stars with comparable metallicities.

Table 1

τ Ceti Parameters

Parameter	Value	Source
Mass ($M_\odot$)	0.69 ± 0.09	**?**
Angular Diameter	2.019 ± 0.012	**?**
Radius ($R_\odot$)	0.793 ± 0.004	**?**
Surface Gravity (log g)	4.48 ± 0.05	**?**
Effective Temperature (K)	5320 ± 40	**?**
Luminosity ($L_\odot$)	0.45 ± 0.02	**?**
Metallicity [Fe/H]	-0.50 ± 0.03	**?**
X	0.718353	**?**
Y	0.275005	**?**
Z	0.006420	**?**
Rotational Velocity (km s^{-1})	0.1 ± 0.1	**?**
Age (Gyr)	12.4	**?**
Microturbulent velocity (km s^{-1})	0.58	**?**

Table **??** presents the adopted stellar parameters of τ Ceti, compiled from recent observational and modeling studies. These parameters play a crucial role in the construction of the MARCS-based atmospheric model. For instance, the stellar mass (Table **??**, row 1) and age (row 12) constrain the evolutionary status of τ Ceti, situating it as an old solar-type dwarf star with an estimated age of about 12.4 Gyr (**?**). The angular diameter (row 2), combined with parallax measurements, allows for an accurate determination of the stellar radius (row 3), while the effective temperature $T_{\text{eff}} = 5320$ K (row 5) and luminosity (row 6) provide key inputs for reproducing the spectral energy distribution (SED) and overall flux calibration (**?**).

The metallicity ([Fe/H] ≈ -0.5, Table **??**, row 7) indicates that τ Ceti is relatively metal-poor compared to the Sun, which has implications for planet formation and chemical abundance studies (**?**). The hydrogen (X, row 8), helium (Y, row 9), and metal (Z, row 10) mass fractions from **?** are consistent with this low-metallicity profile and serve as input for opacity and equation-of-state calculations within the model. Surface gravity (log $g = 4.48$, row 4) and microturbulent velocity (row 13) are critical for fitting individual spectral lines, particularly those sensitive to pressure broadening and small-scale turbulent motions (**?**).

Together, these parameters establish a coherent framework for atmospheric modeling, ensuring that the synthetic spectra generated with the MARCS grid and the SPECTRUM code can be reliably compared with observations. In this way, the parameter set provides a foundation not only for the present analysis of τ Ceti but also for comparative studies of nearby solar analogs and metal-poor stars.

Table 2

MARCS Input Grid Parameters for τ Ceti

Physical Parameters	Minimum	Maximum
Effective Temperature (K)	5320	5500
Log g	4.5	5
Fe/H	-0.5	-2.5
ξ (km/s)	0	1

3. METHODS

The atmospheric modeling was carried out using the Model Atmospheres with a Radiative and Convective Scheme (MARCS) by **?**. This program is a one-dimensional hydrostatic stellar atmosphere grid model, either plane-parallel or spherical, adopting mixing length convection and Local Thermodynamic Equilibrium (LTE). MARCS provides 52 000 atmospheric models, primarily for cool stars of classes F, G, K, M, as well as carbon stars and population II stars with specific metallicities. Therefore, this program is suitable for τ Ceti, which is classified as a cool and metal-poor star. The MARCS model parameters include: Temperature ranging from 2500 to 8000 K (step 100 K for 2500 to 4000 K and 250 K for 4000 to 8000 K), Surface gravity ranging from 0 to 5 (step 0.5), [Fe/H] values ranging from -5 to 1 (with variable steps), microturbulence velocity 0 to 5 km/s.

The atmospheric model constructed for τ Ceti uses a plane-parallel geometry model, which is appropriate for cool stars, with log g values only between 3.5 and 5, along with the input parameters needed to obtain the grid data presented in Table 2. These parameters can be directly entered on the website http://marcs.astro.uu.se, and the four ASCII output files with extensions ".mod", ".opa", ".krz", and ".fix" can be downloaded from the site. These files contain thermodynamic quantities compiled using gfortran for the purposes of analysis and spectral synthesis. With the input parameters listed in Table 2, a total of eight grid data sets were obtainain the atmospheric model with the effective temperature, log g, and metallicity that match the fundamental parameters of τ Ceti, interpolation was performed from the MARCS grid boundaries given in Table 2. The input parameters correspond to the fundamental values of τ Ceti: $T_{\text{eff}} = 5373$ K, log g = 4.44, and [Fe / H] = –0.49. The interpolated output files with the extensions ".interpol" and ".alt" contain thermodynamic quantities that are used to construct the stellar atmosphere model.

Subsequently, in addition to their application in constructing atmospheric models, the interpolated parameters are employed to generate synthetic spectra. The spectra synthesis is carried out using the SPECTRUM program developed by **?**. Spectrum is available for download as a tarred-gzipped file on http://www.phys.appstate.

edu/spectrum/spectrum.html. The resulting spectra are compared with observational spectroscopic data. The parameters adopted for constructing the spectral profiles include mass depth, temperature, gas pressure, electron density, opacity, radiation pressure, and microturbulent velocity.

4. RESULT

4.1. ATMOSPHERIC MODEL

The following are curves of several thermodynamic quantities as a function of τ Rosseland obtained from interpolation using MARCS.

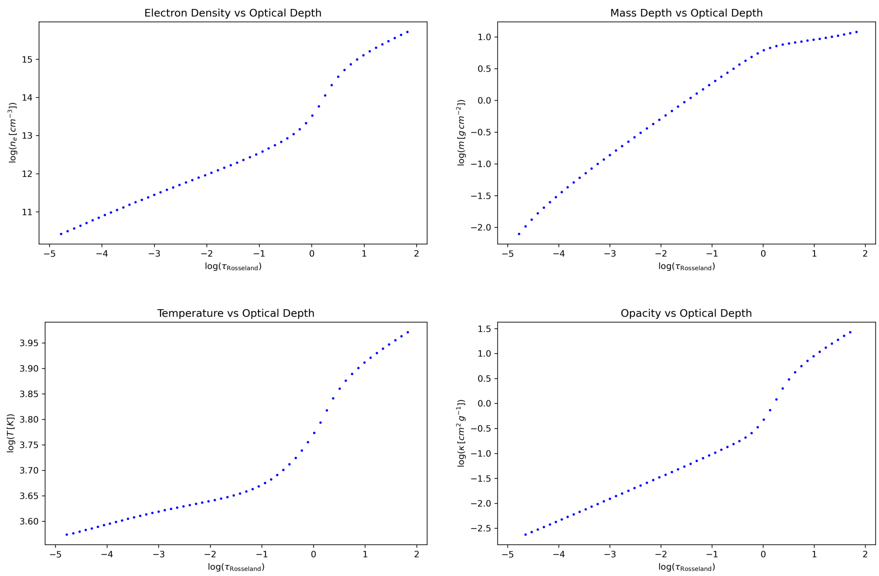

Fig. 1 – Thermodynamic structure of the stellar atmosphere, showing electron density, mass depth, temperature, and opacity as functions of Rosseland optical depth (τ_{Ross}), based on interpolated MARCS model outputs.

Figure **??** illustrates the variation of electron density, mass depth, temperature, and the Rosseland mean absorption coefficient (κ_{Ross}) as functions of Rosseland optical depth (τ_{Ross}). Increasing values of τ_{Ross} (toward the right on the x-axis) correspond to progressively deeper atmospheric layers approaching the stellar interior. Overall, all parameters display a monotonic increase with optical depth, consistent with theoretical expectations for radiative equilibrium stellar atmospheres (**??**).

In the top two panels, the plots demonstrate that deeper layers exhibit both higher mass depth and greater electron density, reflecting enhanced ionization in high-temperature regions (?). The temperature profile increases gradually for $\log \tau_{\rm Ross} \lesssim -1$, followed by a steeper rise at larger optical depths. Notably, the point where the temperature equals the effective temperature of τ Ceti ($T_{\rm eff} = 5373$ K) occurs at $\tau_{\rm Ross} \approx 2/3$ ($\log \tau_{\rm Ross} \approx -0.17$), a standard depth defining the photosphere–atmosphere boundary in classical model atmospheres (?).

The bottom-right panel shows the Rosseland mean opacity ($\kappa_{\rm Ross}$), which increases with depth, indicating that material density and ionization fraction both rise toward the stellar interior. This trend is a hallmark of late-type dwarf stars, where opacity sources are dominated by contributions from bound-free and free-free transitions (?).

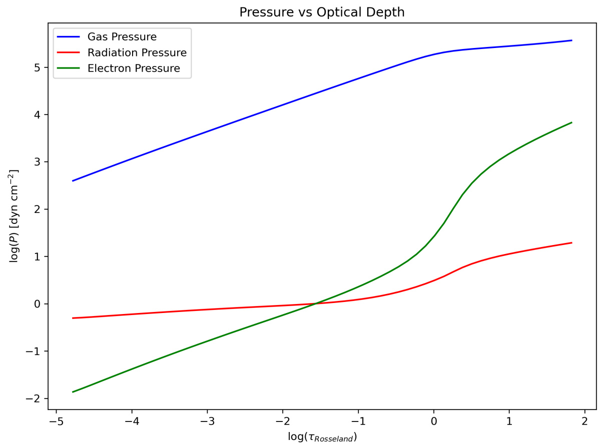

Fig. 2 – Plot of Gas Pressure (blue), Radiation Pressure (red), and Electron Pressure (green) as functions of τ Rosseland.

Figure ?? illustrates the variation of different pressure components as a function of Rosseland optical depth ($\tau_{\rm Ross}$), including the gas pressure ($P_{\rm gas}$), radiation pressure ($P_{\rm rad}$)-arising from the radiative transfer of energy by photons-and the electron pressure (P_e). Similar to Figure ??, all three curves display a general increase with optical depth, reflecting that deeper layers in the stellar atmosphere experience higher pressure values (??). The radiation pressure (red curve) rises relatively slowly in the outer atmosphere and then steepens toward the interior, consistent with enhanced radiative processes in high-density layers. The electron pressure (green curve) shows a more pronounced increase in deeper regions, particularly beyond $\tau_{\rm Ross} = 1$, reflecting higher ionization fractions in the stellar interior (?). Both radiation and electron pressures converge at approximately 1 dyne cm^{-2} near $\tau_{\rm Ross} \approx 0.03$ ($\log \tau_{\rm Ross} \approx -1.5$). The gas pressure (blue curve) dominates throughout the atmosphere, exhibiting a sharp rise in the outer layers up to $\tau_{\rm Ross} \lesssim 1$, followed by a steady increase toward the

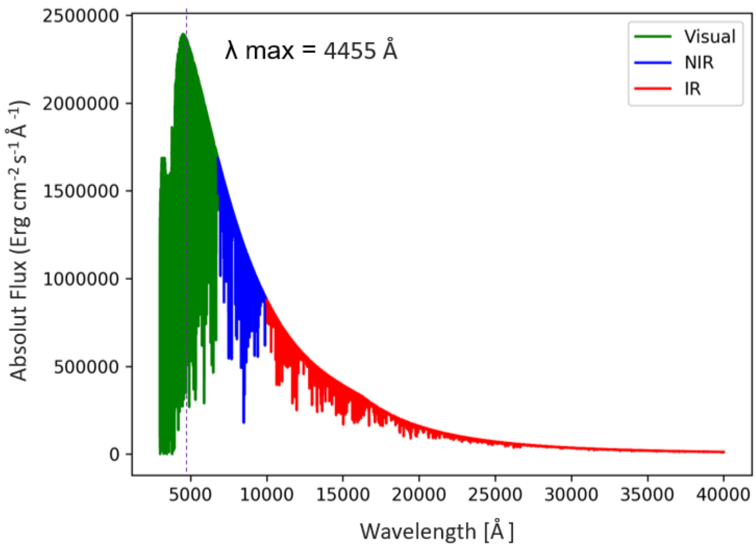

Fig. 3 – Spectral Energy Distribution (SED) of τ Ceti generated using the SPECTRUM code with a MARCS model atmosphere

stellar interior, consistent with hydrostatic equilibrium conditions in late-type dwarf stars (**??**).

4.2. SYNTHETIC SPECTRA

The atmospheric model provides a self-consistent description of the stratification of temperature, density, and pressure throughout τ Ceti's atmosphere, establishing a robust framework for further analysis. Leveraging these results, synthetic spectra were computed to directly connect the theoretical structure with observational data, enabling a rigorous evaluation of the model's predictive capability and offering refined constraints on the star's physical parameters. Figure **??** presents the spectral energy distribution (SED) of τ Ceti, generated using the `SPECTRUM` program based on the interpolated MARCS model atmosphere. The flux is shown as a function of wavelength, expressed in units of $\mathrm{erg\,cm^{-2}\,s^{-1}\,\AA^{-1}}$. The distribution exhibits a clear maximum at $\lambda_{\max} = 4455\,\AA$, which lies in the visual domain (green region). At longer wavelengths, the flux gradually decreases, extending through the near-infrared (blue) and infrared (red) regions. This profile reflects the blackbody-like behavior of stellar radiation modified by atmospheric absorption features, and it provides a useful reference for comparison with observed spectra of solar-type stars.

Figure **??** shows the comparison between the synthetic spectrum of τ Ceti, computed with SPECTRUM, and the observational data reported by **?**. The observations were obtained with the Coudé Echelle Spectrograph (CES) at the ESO 1.4-m Coudé Auxiliary Telescope (CAT), using a Reticon detector. Three representative wavelength regions are presented: 525.7–527.6 nm (top left), 588.1–590.5 nm (top right), and 614.3–616.5 nm (bottom). Within these intervals, key diagnostic features can be identified, namely the Fe I line at $\lambda = 526.955$ nm, the Na I D line at $\lambda = 588.995$ nm, and the Ca I line at $\lambda = 616.217$ nm.

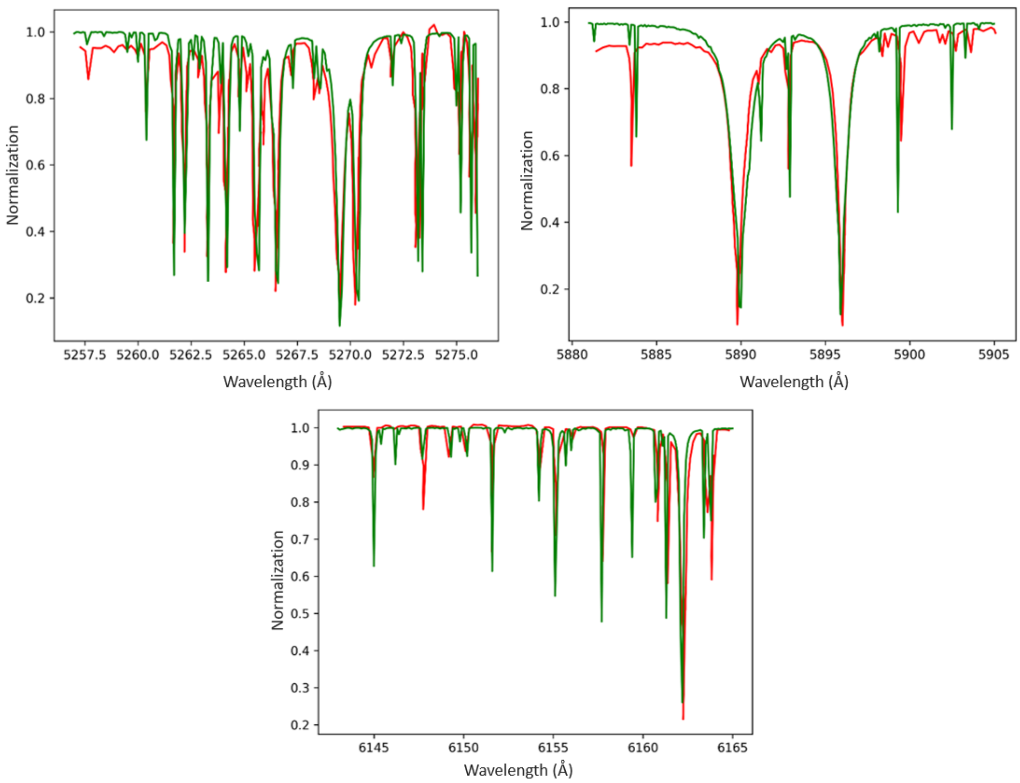

Fig. 4 – Comparison between the observed (green) and synthetic (red) spectra of τ Ceti in three selected wavelength regions. The panels show (top left) the Fe I line around 526.955 nm, (top right) the Na I D line around 588.995 nm, and (bottom) the Ca I line around 616.217 nm.

The comparison demonstrates that the synthetic profiles (red) reproduce the overall shape and depth of the observed spectra (green) with satisfactory agreement. Although minor discrepancies are visible in line depths and wings, the general consistency supports the reliability of the atmospheric model. These specific absorption features are of particular importance, as they serve as diagnostics for constraining the stellar surface gravity and other fundamental parameters of τ Ceti (**?**).

5. DISCUSSION AND SUMMARY

The atmospheric model constructed for τ Ceti through interpolation of the MARCS grid provides valuable insights into the star's physical structure by resolving the stratification of fundamental thermodynamic quantities, including mass depth, temperature, gas and electron pressure, and opacity. These parameters exhibit systematic variations with Rosseland optical depth, increasing toward the stellar interior, consistent with theoretical expectations for stars in hydrostatic equilibrium (**??**). The steep temperature gradient observed at $\tau_{\mathrm{Ross}} \gtrsim 1$ reflects the transition from radiative to deeper convective layers, while the pressure stratification highlights the dominance of gas pressure over radiation pressure in late-type dwarf stars (**?**). Notably, the results confirm that τ Ceti's atmosphere is representative of a metal-poor, solar-type dwarf star, with physical conditions that make it an excellent benchmark for testing stellar atmosphere models and spectroscopic diagnostics.

Such modeling not only captures the physical state of the outer stellar layers but also provides a robust framework for interpreting spectral diagnostics, as atmospheric structure strongly influences both line formation and continuum opacity. This detailed characterization serves as a foundation for generating synthetic spectra and validating model predictions against high-resolution observations. By linking atmospheric models with spectroscopic measurements, this approach enables precise determinations of fundamental stellar parameters and chemical abundances, contributing to improved benchmarks for solar-type and metal-poor stars in galactic studies.

Acknowledgements. This research has made use of the MARCS model atmosphere grid (**?**) and the SPECTRUM spectral synthesis code (**?**). The authors gratefully acknowledge the developers and maintainers of these software packages for making their tools publicly available to the scientific community. We also thank the anonymous editor and reviewer for their constructive comments that helped improve the manuscript.
The authors would also like to express their gratitude to the lecturer of the Stellar Physics course during the graduate program in Astronomy at ITB, whose teachings provided a strong foundation for this work.

REFERENCES

Arribas, S. and Crivellari, L.: 1989, *Astron. Astrophys.* **210**, 211.

Attrill, G., Nakwacki, M.S., Harra, L.K., van Driel-Gesztelyi, L., Mandrini, C.H., Dasso, S. and Wang, J.: 2006, *Solar Phys.* **238**, 117.

Baum, A.C., Wright, J.T., Luhn, J.K. and Isaacson, H.: 2022, *Astron. J.* **163**, 183.

Di Folco, E., Kervella, P., Morel, P., Thévenin, F., de Souza, A.D. and du Foresto, V.C.: 2004, *Astron. Astrophys.* **426**, 601.

Di Folco, E., Pericaud, J., Augereau, J.C. and Marshall, J.: 2014, in *Proc. SF2A-2014*, eds. Ballet, J., Martins, F., Bournaud, F., Monier, R., and Reylé, C., Paris, France, 177.

Feng, F., Tuomi, M., Jones, H.R.A., Barnes, J., Anglada-Escudé, G., Vogt, S.S. and Butler, R.P.: 2017, *Astron. J.* **154**, 135.

Greaves, J. S., Wyatt, M. C., Holland, W. S., Dent, W. R. F.: 2004, Mon. Not. R. Astron. Soc., **351**, 3, L54.

Gray, D.F.: 2005, *The Observation and Analysis of Stellar Photospheres*, 3rd edn., Cambridge University Press, Cambridge.

Gray, R.O.: 2010, Documentation for SPECTRUM v2.76, http://www.appstate.edu/~grayro/spectrum/spectrum.html.

Gustafsson, B., Edvardsson, B., Eriksson, K., Jørgensen, U.G., Nordlund, Å. and Plez, B.: 2008, *Astron. Astrophys.* **486**, 951.

Hubeny, I. and Mihalas, D.: 2014, *Theory of Stellar Atmospheres: An Introduction to Astrophysical Non-equilibrium Quantitative Spectroscopic Analysis*, Princeton University Press, Princeton.

Korolik, M., Roettenbacher, R.M., Fischer, D.A., Kane, S.R., Perkins, J.M., Monnier, J.D., Davies, C.L., Kraus, S., Le Bouquin, J.B. and Narsireddy, P.: 2023, *Astron. J.* **166**, 123.

Lawler, S.M., Di Francesco, J., Kennedy, G.M., Matthews, B.C. and Greaves, J.S.: 2014, *Mon. Not. R. Astron. Soc.* **444**, 2665.

MacGregor M. A., Lawler S. M., Wilner D. J., Matthews B. C., Kennedy G. M., Booth M., Di Francesco J.: 2016, Astrophys. J., **828**, 113.

Mumtahana, F.: 2020, *J. Phys. Conf. Ser.* **1523**, 012012.

Pagano, M., Truitt, A., Young, A.P. and Shim, S.H.: 2015, *Astrophys. J.* **803**, 90.

Paxton, B., Cantiello, M., Arras, P., Brown, E.F., Dotter, A., Mankovich, C., Montgomery, M.H., Stello, D., Timmes, F.X. and Townsend, R.H.D.: 2013, *Astrophys. J. Suppl. Ser.* **208**, 4.

Pavlenko, Ya.V., Jenkins, J.S., Jones, H.R.A., Ivanyuk, O. and Pinfield, D.J.: 2012, *arXiv e-prints*, arXiv:1201.5099.

Pijpers, F.P., Teixeira, T.C., Garcia, P.J., Cunha, M.S., Monteiro, M.J.P.F.G. and Christensen-Dalsgaard, J.: 2003, *Astron. Astrophys.* **406**, L15.

Tang, Y.K. and Gai, N.: 2011, *Astron. Astrophys.* **526**, A35.

Teixeira, T.C., Kjeldsen, H., Bedding, T.R., Bouchy, F., Christensen-Dalsgaard, J., Cunha, M.S., Dall, T., Frandsen, S., Karoff, C., Monteiro, M.J.P.F.G. and Pijpers, F.P.: 2009, *Astron. Astrophys.* **494**, 237.

Tucci Maia, M., Meléndez, J. and Spina, L.: 2019, *Astron. Astrophys.* **628**, A126.

Tuomi, M., Jones, H.R.A., Jenkins, J.S., Tinney, C.G., Butler, R.P., Vogt, S.S., Barnes, J.R., Wittenmyer, R.A., O'Toole, S.J., Hoener, J., Bailey, J., Carter, B.D., Wright, D.J., Salter, G.S. and Pinfield, D.J.: 2013, *Astron. Astrophys.* **551**, A79.

Received on 10 Sep 2025